Development of hybrid scaffold bioactive glass nanoparticles/chitosan for tissue engineering applications

Hassane Oudadesse, Sanaa Najem, Siwar Mosbahi, Nicolas Rocton, Jihen Refifi, Hafedh El Feki, Bertrand Lefeuvre

ORIGINAL ARTICLE

Development of hybrid scaffold: Bioactive glass nanoparticles/chitosan for tissue engineering applications

Hassane Oudadesse [1,*] | **Sanaa Najem** [1] | **Siwar Mosbahi** [1] | **Nicolas Rocton** [1] | **Jihen Refi fi** [1,2] | **Hafedh El Feki** [2] | **Bertrand Lefeuvre** [1]

[1] Univ Rennes, CNRS, ISCR-UMR 6226, Rennes, France

[2] Faculty of Science, University of Sfax, Sfax, Tunisia

Correspondence
Hassane Oudadesse, Univ Rennes, CNRS, ISCR-UMR 6226, F-35000 Rennes, France.
Email: hassane.oudadesse@univ-rennes1.fr

Funding Information
CNRS
Université de Rennes 1

Abstract

Bone tissue engineering is gaining popularity as an alternative method for the treatment of osseous defects. A number of biodegradable polymers have been explored for tissue engineering purposes. A new family of biodegradable polymer/bioactive glass composite materials has been designed to be used in bone regeneration approaches. In this work, a hybrid scaffold of chitosan (CH) and bioactive glass nanoparticles (BGN) was prepared by the freeze-gelation method. This method has been studied by adjusting the concentration of acetic acid; this process can influence the structure properties of the scaffold. In this work, several BGN/CH composites have been prepared by varying the proportion of BGN in the hybrid scaffold (20, 40, 60, and 80%). Brunauer–Emmett–Teller results showed the increased surface area and porosity volume of our composite with decreasing BGN proportion. BGN/CH hybrid scaffold was characterized by using physicochemical techniques. Obtained results showed a macroporous morphology of the scaffold with a pore size of about 200 μm, and a homogeneous distribution of the BGN in the CH matrix. X-ray diffraction study confirmed the amorphous state of the BGN/CH hybrid scaffold. Interaction between CH and BGNs in the composite was confirmed. The in vitro assays showed adequate degradation properties, which is essential for the potential replacement by the new tissue. The in vitro bioactivity studies confirmed the formation of an apatite layer on the surface of the hybrid scaffold, which results in a direct bone bonding of the implant. These results indicate that BGN/CH hybrid scaffold developed is a potential candidate for bone tissue engineering.

Keywords

chemical reactivity | chitosan | hybrid biomaterial | nano bioactive

glass | porosity | scaffold

1INTRODUCTION

The tissue engineering domain is a promising research field for bone biomaterials development. Natural implants and synthetic biomaterials are used to repair human body parts and to restore their biological functions. An ideal implant for the regeneration of damaged tissues is a synthetic porous material. In our research group, we focused on porous glass ceramics and. The scaffold is a material that presents a homogeneous and organized porosity in its three-dimensional (3D) architecture and in the form of stratified layers.

These scaffolds combined with organic molecules, bisphosphonates such as clodronate, risedronate, raloxifene, and/or biopolymers are able to play double functions: regeneration of bone tissue and contribution of certain bone pathologies by drug delivery. Then they contribute to being resorbed after a certain period of their insertion in bone sites (Balanta, 2014; Jones, 2013; Mozafari & Moztarzadeh, 2014). For the development of an optimal scaffold, we adopted the necessity of stable direct contact between bone and the scaffold surface as a critical requirement. Excellent biocompatibility, a controllable biodegradability, and an adapted mechanical strength were used capital properties for an ideal scaffold used for several applications in tissue engineering.

Several biodegradable polymers such as poly(caprolactone), poly(vinyl alcohol), and natural polymers such as collagen and biopolymers like chitosan (Hirano et al., 1990) are used in the biomaterials field. They demonstrated their positive effect on bone restoration. Chitosan is a natural biopolymer extracted from the chitin by a partial chemical or enzymatic deacetylation. Our previous works demonstrated its effect on the osteoporosis phenomenon when it is associated with bioactive glass biomaterials. Chitosan represents an ideal material for uses in tissue engineering because of its several biological characteristics such as its good biocompatibility, biodegradability, bioinert, and its capacity to adsorb such protein (Gupta, Mahor, Khatri, Goyal, & Vyas, 2006; Jayakumar, Nwe, Tokura, & Tamura, 2007; Jayakumar, Prabaharan, Reis, & Mano, 2005; Jayakumar, Reis, & Mano, 2006; Jayakumar, Selvamurugan, Nair, Tokura, & Tamura, 2008; Muzzarelli, 2009; Muzzarelli et al., 1988). Its chemical composition, which resembles a major component of the bone and cartilaginous tissue, encourages the cell adhesion.

Thinks to its cationic nature, chitosan can form complexes with anionic macromolecules such as glycosaminoglycan, which regulate the cytokines and growth factors activity. Its contribution on cell proliferation and differentiation was evidenced (Aranaz et al., 2009; Di Martino, Sittinger, & Risbud, 2005; Şenel & McClure, 2004; Seol et al., 2004).

Several synthetic materials such as calcium phosphate in the form of hydroxyapatite (Jayakumar & Tamura, 2006; Jiang, Nair, & Laurencen, 2006; Kong et al., 2005; Zhang et al., 2008; Zhao, Grayson, Ma, Bunnell, & Lu, 2006), or ß-tricalcium phosphate, or calcium phosphate and geopolymers (Takahashi, Yamamoto, & Tabata, 2005; Yin et al., 2003; Zheng

et al., 2007) pure, doped with atomic elements or associated with organic molecules have been investigated.

Previous studies demonstrate the good effect of the chitosan/bioactive glass association in the improvement of the biological and chemical properties of the obtained composite. In fact, chitosan through its chemical nature approves the cell attachment and bioactive glass enhances the chemical property of this composite (Dorj, Park, & Kim, 2012; Hunger, Donius, & Wegst, 2013).

Bioactive glass represents a good candidate for biomedical devices thanks to several properties such as biocompatibility, bioactivity, and its ability to form good chemical links between the biomaterial and the surrounding tissue (Berthiaume, Maguire, & Yarmush, 2011; Jones, 2013; Rahaman et al., 2011).

Our previous works have been based on the preparation of bioactive composite glass and chitosan biopolymer (17%) by the freeze-drying process. Through their in vivo experiments, we studied its antioxidative performance and its effect of the generated porosity in the resorption and in the osseointegration of the obtained bio composite (Bui, Oudadesse, Le Gal, Merdrignac-Conanec, & Cathelineau, 2012; Jebahi et al., 2014; Oudadesse et al., 2013).

Usually, by comparison to the microphase ceramics, the interaction between cell and material was well reported on the surface of nanophase ceramics (Webster, 2000). Using nano bioactive glass aimed to enhance the mechanical and biological performance of scaffolds. Improvement of bone cells such as osteoblasts and their effect on the scaffold substrate encourage their use as bone biomaterials (Alves, Leonor, Azevedo, Reis, & Mano, 2010). Thus, several studies aimed to develop specific methods for the synthesis of porous scaffold. They were based on the introduction of porogen leaching in the structure of the material (Chen, Ushida, & Tateishi, 2000; Chen, Ushida, & Tateishi, 2001; Ma, Wang, He, & Chen, 2001), the release of CO_2 (Harris, Kim, & Mooney, 1998; Mooney, Baldwin, Suh, Vacanti, & Langer, 1996), 3D printing (Park et al., 1997), and phase separation mechanisms (Han, 2000; Nam & Park, 1999; Schugens, Maquet, Grandfils, Jerome, & Teyssie, 1996a; Schugens, Maquet, Grandfils, Jerome, & Teyssie, 1996b; Whang, Thomas, Healy, & Nuber, 1995). The well-employed method is the thermally induced phase separation (TIPS) (Ma et al., 2001; Nam & Park,1999; Whang et al., 1995). This method is based on the decrease of solution temperature in order to generate the homogeneous biodegradable polymer solution phase separation. It can induce polymer-poor phase and polymer-rich liquid phase (Han, 2000). The growing and coalescence of the polymer-poor phase allow the introduction of multiple pores in scaffolds. When the temperature was well attenuated and lead to the solution freezes, we obtained the separation phase between solid and liquid that formed frozen solvent and polymer-rich phases. Finally, the frozen solvent removal leaves place for pores.

Our study believed that the freeze-gelation process is very important in terms of either energy and time, very easy to employ, and produces less residual solvent. For that, it was well used in the development of scaffold material. This new technique was well evaluated through the regulation of several parameters such as the freezing temperature, and both acetic acid and ethanol concentrations in the gelation environment. Scaffold architecture is very essential for tissue engineering development. In the freeze-gelation technique, several parameters can influence the scaffold structure. Over the freezing technique, the temperature decrease leads to the formation of the phase separation permitting the apparition of ice and chitosan-rich

phases. At the phase separation step, the scaffold porosity, architecture, and characteristics are defined. Thus, the freezing temperature of the BGN/CH solution is an essential variable parameter. At the gelation step, chitosan phases undergo condensation phenomena and the ice left its place for the creation of pores after the lyophilization process.

In the present work, the chitosan solution was prepared after its dissolving in the acetic acid solvent, which constitutes another variable parameter. In this study, the development of the sol–gel technique has been adapted for the elaboration of bioactive glass nanoparticles. The chitosan/bioactive glass nanoparticles (BGNs) as a hybrid scaffold was prepared by the freeze-gelation method based on the TIPS. This composite scaffold was characterized, and its bioactivity and biodegradability have been studied relevant to biomedical applications.

2EXPERIMENTAL PROCEDURE

2.1Synthesis of BGN and the BGN/CH (20:80) hybrid scaffolds

The sol–gel process was used for the synthesis of the BGN (SiO_2:CaO:P_2O_5 [mol] = 55:40:5). Calcium nitrate solution and tetraethylorthosilicate (TEOS) were blended and then followed by the addition of the citric acid in the goal to fix the pH value to 1–2. Under, vigorous agitation, the obtained solution was slowly supplemented to the solution of ammonium dibasic phosphate. Over the dropping step, the pH of the solution was adjusted to a value of around 10–11, employing the NH_3 solution.

After 48 hr of agitation and 24 hr of maturation, the solution was centrifuged leading to the separation between the precipitate and initial product in a 200 ml of 2% PEG-water solution. The obtained powder was lyophilized for 48 hr and followed by its calcination at 600°C for 3 hr. Finally, we obtained our BGN powder.

This work detailed the hybrid porous scaffolds BGN/CH employing newly developed freeze-gelation process. The freeze-gelation is based on the principle of thermally induced phase separation (Figure 1). Two percent of polymer solution was obtained by the dissolving chitosan in an acetic acid aqueous solution (1 *M*). Nano bioactive glass particles (0.4%) were suspended in the deionized water for 1 hr under ultrasonication.

FIGURE 1 Schematic representation of bioactive glass nanoparticle (BGN)/chitosan (CH) composite scaffold fabrication method (freeze-gelation)

The suspension was added to the previously prepared chitosan solution. Then, the chitosan/BGN suspension was put at −20°C, in a Petri dish, during 24 hr (Bi et al., 2011).

The frozen sample was soaked in a solution of NaOH/ethanol in the goal to adapt its pH value in order to permit the chitosan gelation. The NaOH/ethanol solution was cooled to −20°C in order to favor the chitosan gelation process below the chitosan freeze point. Indeed, the NaOH aqueous solution leads to the alkalinity for gelation and the ethanol leads to decrease in the freezing point. Prepared porous composite scaffold (BGN/CH) through freeze-gelation and after freeze-drying processes is presented in Figure 2.

FIGURE 2 Image of the porous bioactive glass nanoparticle (BGN)/chitosan (CH) composite scaffold prepared by the freeze-gelation method after freeze-drying

The success of elaborated scaffolds for use as filling biomaterials depends on the porous structure and architecture. The freeze-gelation technique contained several processes, which influence scaffolds structure. In the present work, we used the acetic acid as a solvent for the preparation of chitosan solution. The acetic acid concentration ranged from 0.2 to 2 *M* and the effect of this variation on the scaffold structure was well detailed.

2.2Morphological evaluation of hybrid scaffolds

The morphological structure of the obtained material (BGN/CH) has been evaluated by scanning electron microscopy (SEM). Before the start of the morphological analysis, samples have been metalized using a layer of gold–palladium.

2.3Functional groups evaluation: Fourier-transform infrared spectroscopy

The Bruker Equinox 55 spectrometer was used for the infrared spectroscopy study. Ten milligrams of dried composite scaffolds were ground and homogenized with KBr powder and pressed in the order to form a suitable pellet for the infrared analysis. Data were collected between 4,000 and 400 $cm^{-1}$and lead to collect the functional groups composed of the hybrid scaffolds.

2.4Structural analysis and surface areas

The powders of the obtained scaffolds were analyzed by X-ray diffraction (XRD) in order to have more information on their structure. XRD diagrams were recorded by using a Panalytical diffractometer (Cu Kα radiation, 40 kV, 30 mA) in the 2θ range of 5°–90° with a step size of 0.026° and counting time of 30 s for each step.

The specific surface area was measured using the Brunauer–Emmett–Teller (BET) N2 adsorption–desorption process (Flowsorb II 2300, Coultronics France SA). The pore volume was also determined.

2.5Chemical reactivity evaluation

The chemical reactivity of the obtained BGN/CH scaffolds was evaluated by soaking of 30 mg of powder in 20 ml of the simulated body fluid (SBF) having the same composition of the blood plasma. Samples were immersed during 1, 3, 5, and 7 days under 37°C and 50 rpm/min to allow the similar conditions of the physiological environment.

SBF composition as presented in our previous works and as described by Kokubo and Takadama (2006)) is shown in Table 1.

TABLE **1**Comparison between ion concentrations (m*M*) in SBF and in human blood plasma

	Na^+	K^+	Ca^{2+}	Mg^{2+}	Cl^-	HCO_3^-	HPO_4^{2-}
SBF	142	5	2.5	1.5	148.8	4.2	1
Blood plasma	142	5	2.5	1.5	103	27	1

After each immersion period, the powder was rinsed with water, and then with alcohol in order to stop the chemical reaction, while the solution was stored in the fridge under 4°C in order to evaluate the chemical exchange between biomaterial and SBF solution.

After its lyophilization, the powder was characterized by several physicochemical techniques such as infrared spectroscopy, XRD, and SEM to allow and understand the chemical reactivity of the immersed biomaterial.

2.6In vitro biodegradation

The in vitro behavior of hybrid BGN/CH was evaluated in phosphate-buffered saline (PBS) under 37°C. Materials with dimensions of 10 × 10 × 2 mm^{-3} were soaked in 10 ml of PBS and were placed with a weak agitation in physiological condition (37°C) for 7 days. PBS chemical composition is detailed in Table 2. PBS solution was formed by the dissociation of NaCl and KCl, Na_2HPO_4 and KH_2PO_4 in an aqueous solution (distilled water) having a pH value of 7.4. The initial weight of scaffolds is called W_i. Following all immersion delays, the material was rinsed with deionized water in order to eliminate all adsorbed ions on the surface and then dried. The dry weight is called W_t. The liberation of scaffold elements in the BPS

solution was measured by the following equation:

TABLE **2**Chemical composition of the phosphate-buffered saline (PBS) medium

	NaCl	**KCl**	**Na_2HPO_4**	**KH_2PO_4**
Reagent concentration (m*M*) in PBS	137	2.7	10	1.8

3RESULTS AND DISCUSSION

3.1Characterizations of the BGN/hybrid scaffold

SEM of the obtained composite (Figure 3) showed that BGN/CH hybrid scaffolds present well-interconnected pores.

FIGURE 3(a, b) Scanning electron micrograph (SEM) showing the macroporous structure of bioactive glass nanoparticle (BGN)/chitosan (CH) composite scaffold (a) and the dispersion of BGN in the matrix (b). Pore size is about 200 μm (b, white arrows)

The size of the obtained scaffolds pores varied from 100 to 300 μm as shown by the SEM analysis. The pore size of the scaffold varied between 100 and 300 μm. As presented in Figure 3, the BGNs are arranged on the walls of the scaffold with homogeneous dispersion. Good adhesion between the BGNs and chitosan biopolymer has been obtained and presented in Figure 3b (white arrows), noting that the cell size is about 10–100 μm. The pore size of the hybrid scaffolds is adapted to cell integration in the interior of the BGN/CH. Pores have a key role in the integration and differentiation of stem cells and also in the process of vascularization. The functions of pores depend on their size. In fact, large pores enhance the osteogenesis, the vascularization, and the oxygenation process. However, the smaller pores assign the osteochondral ossification. Also, the geometry of pores varied the type of growth factor present in the biomaterial (Karageorgiou & Kaplan, 2005). There are two benefits if using freeze-drying to remove the solvent: the first is to keep the temperature low enough that the polymer-rich region would not dissolve again and the second is to possess enough mechanical strength through the ice to prevent pore collapse during drying (Ho et al., 2004).

The XRD diagrams and thermal curve underline the amorphous structure of BGN (Figures 4 and 5). In fact, nano bioactive glass illustrates the presence of only a diffraction halo observed between 15° and 40° (2θ) (Madhumathi et al., 2009) (Figure 4). The vitreous temperature of nano bioactive glass is 660°C (Figure 5). XRD of chitosan scaffold presents a peak at 21°. The diagram of the hybrid BGN/CH underlined the appearance of a new peak at 21° (2θ) this peak was replaced by a diffraction halo in the XRD pattern of BGN/CH hybrid scaffold. The disappearance of the chitosan peak in the XRD pattern of the composite confirmed its amorphous state and demonstrated the interaction between the BGNs and chitosan.

FIGURE 4X-ray diffraction (XRD) pattern of (a) bioactive glass nanoparticle (BGN), (b) chitosan, and (c) BGN/CH composite scaffold

FIGURE 5 Thermal analysis (DSC) of nano bioactive glass

FTIR spectra of the BGN/CH hybrid scaffold (Figure 6c) showed the presence of bands at 1,649 and 1,420 cm^{-1}. These bands underlined the first amine group and the secondary amine groups of chitosan, respectively. As compared to the chitosan, the hybrid scaffold (BGN/CH) showed the presence of two bands of P-O observed at 602 and 564 cm^{-1} and a band of Si─O─Si observed at 467cm^{-1}. In comparison to the FTIR spectra of BGN, the composite presents two peaks, which correspond to amine groups and modification in Si─O─Si band. The presence of amine groups and the modification in the silicate band can be attributed to the interactions between the BGN and the chitosan. The broadband in the FTIR spectra of BGN (Figure 6a), from 3,100 to 3,470 cm^{-1}, corresponding to the O─H stretching absorption band was modified in the spectra of BGN/CH. The aliphatic C─H stretching band in the FTIR spectra of chitosan (Figure 6b) observed between 2,885 and 2,990 cm^{-1} disappears from the spectra of BGN/CH. The modification of peaks in the hybrid scaffold spectra confirmed that a chemical bond has taken place between the components. The bonding between chitosan and

bioactive glass was assisted by the existence of silanol groups (Si─OH) in bioactive glass structure and surface as shown in Figure 7.

FIGURE 6 Fourier-transform infrared spectroscopy (FTIR) spectra of (a) bioactive glass nanoparticle (BGN), (b) chitosan, and (c) BGN/CH composite scaffold

FIGURE 7 Representation of chemical interaction between chitosan and bioactive glass nanoparticles

3.2Effect of BGN proportion on the surface area of BGN/CH hybrid scaffold

Different amounts of BGN (20, 40, 60, and 80%) have been employed to synthesize BGB/CH by freeze-gelation method. The surface area and the porosity volume have been measured for the different composites by the BET method. The obtained results showed that for the hybrid scaffold BGN/CH with 20% of BGN the surface area is of about 26.63 m^2/g. The surface area of the hybrid scaffold decreases to 13.81 m^2/g with increasing of BGN amount to 80%. The same variations have been observed concerning the porosity volume. The porosity volume decreases from 7.60 to 6.10 mm^3/g with increasing of BGN amount to 80%. These results were related to the results obtained in the literature, which show the increase of the surface area of the composite with the increasing chitosan amount. The obtained results are summarized in Table 3.

TABLE **3**Surface area and porosity volume obtained by Brunauer–Emmett–Teller (BET) for the different bioactive glass nanoparticle (BGN)/chitosan (CH) composite scaffolds

BGN/CH composite	**Surface area (m^2/g)**	**Porosity volume (mm^3/g)**
BGN 20/CH	26.6 ± 0.4	7.60 ± 0.03
BGN 40/CH	25.3 ± 0.3	6.90 ± 0.04
BGN 60/CH	20.6 ± 0.4	6.70 ± 0.08
BGN 80/CH	13.8 ± 0.3	6.10 ± 0.08

3.3Effect of the acetic acid concentration on the structural behavior of BGN/CH hybrid scaffold

To study the effect of the changes in acetic acid concentration on the structural properties of the BGN/CH hybrid scaffold, two acid concentrations were used: 2 and 0.5 *M*. The SEM micrograph of BGN/CH prepared by 2 *M* acetic acid concentration showed destruction in porous structure and the scaffold was not entirely porous as shown in Figure 8. During the

gelation step of hybrid scaffold preparation, the acetic acid is neutralized by the NaOH solution; this neutralization reaction is the exothermic reaction. The heat release induced the melting of the scaffold and the collapse of the porous morphology of BGN/CH. The amount of heat release increases with increase of acetic acid concentration. Therefore, when we used a lower concentration of acetic acid during the freeze-gelation method, the amount of heat release was low and we obtained a BGN/CH hybrid scaffold with a good organization of porous structure as shown in Figure 8b. Indeed, the obtained porous structure of the scaffolds is very important for medical applications (Chesnutt et al., 2009; Jiang et al., 2008; Slivka, Leatherbury, Kieswetter, & Niederaur, 2002). In fact, the architecture of the pore enhances the integration and the differentiation of stem cells, mesenchymal cells, osteoblasts, and then the vascularization.

FIGURE 8(a, b) Scanning electron micrograph (SEM) showing the structure of bioactive glass nanoparticle (BGN)/chitosan (CH) composite prepared with 2 *M* (a) and 0.5 *M* (b) of acetic acid concentration

3.4In vitro bioactivity study of BGN/CH hybrid scaffold

The bioactivity of the BGN/CH has been tested. Scaffolds have been soaked in SBF solution at different periods from 1 to 7 days. The XRD studies of the hybrid scaffold (Figure 9) after 1 day of immersion showed two peaks at 31° and 45° (2θ) corresponding to hydroxyapatite (Madhumathi et al., 2009); the intensities of these peaks increase with the immersion time, during our study period of 7 days. To analyze the evolution of mineral deposits with immersion time in SBF, the ratio of peak intensities was calculated. Figure 10 showed the evolution of the ratio of intensities depending on the time immersion of the hybrid scaffold in SBF. This ratio increased from 1.48 after 1 day of immersion to 2.13 after 7 days of immersion. The deposition of minerals on the surface of biomaterials amounted to the rise of soaking times in the SBF solution. The BGN/CH bioactivity was justified by the presence of the hydroxyapatite layer at its surface after 7 days of incubation as shown in Figure 11a,b. The presence of this apatite layer on the surface of hybrid scaffolds underlines their chemical reactivity and ability to form a biological link with the surrounding environment. These data highlight the good use of this material for biomedical application. Figure 12a,b shows the in vitro degradation of the BGN/CH hybrid scaffold after 7 days of soaking in the BPS. From 1 to 7 days of soaking, the degradation rate of BGN/CH increases from 2.5 to 9%.
Figure 12b showed the degradation rate of the pure chitosan scaffold for different times of incubation in PBS. The degradation rate increases from 15.3% after 1 day of immersion to 28.5% after 7 days of soaking. BGN/CH hybrid scaffold showed a significant decline in the degradation rate compared to the pure chitosan scaffold. Indeed, the porosity of these hybrid scaffolds enhances the penetration of the PBS solution within the porous structure of chitosan and makes degradation easier. The rate of resorption and degradation of biomaterials is an essential property for the bone graft evaluation. The dissociation of the ß-1,4-N-acetyl glucosamine groups of chitosan chains is provided by lysozyme. The dissociation of the ß-1,4-N-acetyl glucosamine groups of chitosan chains is provided by lysozyme. This process results from the liberation of amino sugars. The association of BGN and chitosan leads to the attenuation of the degradation rate, which was explained by the neutralization of the dissociation of the chitosan acidic product, by the alkali groups of the BGN (Silver, Deas, & Erecińska, 2001).

FIGURE 9X-ray diffraction (XRD) pattern of bioactive glass nanoparticle (BGN)/chitosan (CH) composite scaffolds before and after soaking 1, 3, and 7 days in simulated body fluid (SBF)

FIGURE 10 Variation of peak intensities ratio according to the immersion time of bioactive glass nanoparticle (BGN)/chitosan (CH) composite in simulated body fluid (SBF)

FIGURE 11(a, b) Scanning electron micrograph (SEM) of bioactive glass nanoparticle (BGN)/chitosan (CH) composite scaffold before (a) and after 7 days of immersion in simulated body fluid (SBF) (b)

FIGURE 12(a, b) in vitro degradation studies, which showed the degradation rate of bioactive glass nanoparticle (BGN)/chitosan (CH) nanocomposite scaffold after 7 days of immersion in phosphate-buffered saline (PBS) (a) and compared with the chitosan scaffold (b)

4CONCLUSIONS

BGN/CH hybrid scaffolds were synthesized using the freeze-gelation method for potential applications as bone graft materials for tissue regeneration. The obtained hybrid scaffolds are macroporous biomaterials with pore size ranged between 150 and 300 μm and sufficient microporosity for cell infiltration. The BGN/CH with 20% of the BGN amount presents a better surface area. Seven days after soaking in the PBS solution, these biodegradable scaffolds lost 9% of their weight. As compared with pure chitosan, the addition of BGN retarded the level of chitosan degradation. The chemical reactivity of the obtained hybrid scaffolds was showed through the deposition of a hydroxyapatite layer at the material surface after its incubation in the SBF solution. In conclusion, the bioactivity of bioactive nanoparticles was enhanced by the addition of chitosan to its structure. These results suggest that BGN/CH hybrid scaffold can also serve for drug delivery and appear to be a promising biomaterial for bone tissue engineering applications.

ACKNOWLEDGMENTS

The authors gratefully acknowledge François Cheviré and Franck Tessier for the X-ray diffraction analysis, Francis Gouttefangeas, Loic Joanny, and Christophe Calers (CMEBA) for scanning electron microscopy analysis, Nathalie Herbert and Odile Merdrignac for the BET analyses. The authors would like to thank Université de Rennes 1 and CNRS, France for their funding support.

CONFLICT OF INTEREST

The authors declare no potential conflict of interest.

REFERENCES

1. Verified

   Alves, N. M., Leonor, I. B., Azevedo, H. S., Reis, R. L., & Mano, J. F. (2010). Designing biomaterials based on biomineralization of bone. *Journal of Materials Chemistry*, 20(15), 2911. https://doi.org/10.1039/b910960a

2. Verified

   Aranaz, I., Mengibar, M., Harris, R., Panos, I., Miralles, B., Acosta, N., … Heras, A. (2009). Functional characterization of chitin and chitosan. *Current Chemical Biology*, 3(2), 203–230. https://doi.org/10.2174/2212796810903020203

3. Un-verified

   Balanta, D. (2014). *Utilización de quitosanoprocedentedelmicelio de Aspergillus Níger y su aplicación en regeneración de tejidos* (MS thesis). Universidaddel Valle, Cali, Colombia.

4. Verified

   Berthiaume, F., Maguire, T. J., & Yarmush, M. L. (2011). Tissue engineering and regenerative medicine: History, progress, and challenges. *Annual Review of Chemical and Biomolecular Engineering*, 2(1), 403–430. https://doi.org/10.1146/annurev-chembioeng-061010-114257

5. Verified

   Bi, L., Cao, Z., Hu, Y., Song, Y., Yu, L., Yang, B., … Han, Y. (2011). Effects of different cross-linking conditions on the properties of genipin-cross-linked chitosan/collagen scaffolds for cartilage tissue engineering. *Journal of Materials Science: Materials in Medicine*, 22(1), 51–62. https://doi.org/10.1007/s10856-010-4177-3

6. Verified

   Bui, X. V., Oudadesse, H., Le Gal, Y., Merdrignac-Conanec, O., & Cathelineau, G. (2012). Bioactivity behaviour of biodegradable material comprising bioactive glass. *Korean Journal of Chemical Engineering*, 29(2), 215–220. https://doi.org/10.1007/s11814-011-0151-0

7. Verified

   Chen, G., Ushida, T., & Tateishi, T. (2000). A biodegradable hybrid sponge nested with collagen microsponges. *Journal of Biomedical Materials Research*, 51, 273–282. https://doi.org/10.1002/(SICI)1097-4636(200008)51:2<273::AID-JBM16>3.0.CO;2-O

8. Verified

   Chen, G., Ushida, T., & Tateishi, T. (2001). Preparation of poly(l-lactic acid) and poly(dl-lactic-co-glycolic acid) foams by use of ice microparticulates. *Biomaterials*, 22(18), 2563–2567. https://doi.org/10.1016/S0142-9612(00)00447-6

9. Verified

   Chesnutt, B. M., Viano, A. M., Yuang, Y., Guda, T., Applefors, M. R., Ong, J. L., … Bumgardner, J. D. (2009). Design and characterization of a novel chitosan/nanocrystalline calcium phosphate composite scaffold for bone

regeneration. *Journal of Biomedical Materials Research*, 88A, 491–502. https://doi.org/10.1002/jbm.a.31878

10. Verified

Di Martino, A., Sittinger, M., & Risbud, M. V. (2005). Chitosan: A versatile biopolymer for orthopaedic tissue-engineering. *Biomaterials*, 26(30), 5983–5990. https://doi.org/10.1016/j.biomaterials.2005.03.016

11. Verified

Dorj, B., Park, J.-H., & Kim, H.-W. (2012). Robocasting chitosan/nanobioactive glass dual-pore structured scaffolds for bone engineering. *Materials Letters*, 73, 119–122. https://doi.org/10.1016/j.matlet.2011.12.107

12. Verified

Gupta, P. N., Mahor, S., Khatri, K., Goyal, A., & Vyas, S. P. (2006). Phospholipid vesicles containing chitosan nanoparticles for oral immunization: preparation and in-vito investigation. *Asian Chitin Journal*, 2, 91–96.

13. Verified

Han, M. J. (2000). Biodegradable membranes for the controlled release of progesterone. 1. Characterization of membrane morphologies coagulated from PLGA/progesterone/DMF solutions. *Journal of Applied Polymer Science*, 75, 60–67. https://doi.org/10.1002/(SICI)1097-4628(20000103)75:1<60::AID-APP7>3.0.CO;2-8

14. Verified

Harris, L. D., Kim, B. S., & Mooney, D. J. (1998). Open pore biodegradable matrices formed with gas foaming. *Journal of Biomedical Materials Research*, 42(3), 396–402. https://doi.org/10.1002/(sici)1097-4636(19981205)42:3<396::aid-jbm7>3.0.co;2-e

15. Verified

Hirano, S., Itakura, C., Seino, H., Akiyama, Y., Nonaka, I., Kanbara, N., & Kawakami, T. (1990). Chitosan as an ingredient for domestic animal feeds. *Journal of Agricultural and Food Chemistry*, 38(5), 1214–1217. https://doi.org/10.1021/jf00095a012

16. Verified

Ho, M.-H., Kuo, P.-Y., Hsieh, H.-J., Hsien, T.-Y., Hou, L.-T., Lai, J.-Y., & Wang, D.-M. (2004). Preparation of porous scaffolds by using freeze-extraction and freeze-gelation methods. *Biomaterials*, 25(1), 129–138. https://doi.org/10.1016/S0142-9612(03)00483-6

17. Verified

Hunger, P. M., Donius, A. E., & Wegst, U. G. K. (2013). Structure–property-processing correlations in freeze-cast composite scaffolds. *Acta Biomaterialia*, 9(5), 6338–6348. https://doi.org/10.1016/j.actbio.2013.01.012

18. Verified

Jayakumar, R., Nwe, N., Tokura, S., & Tamura, H. (2007). Sulfated chitin and chitosan as novel biomaterials. *International Journal of Biological Macromolecules*, 40(3), 175–181. https://doi.org/10.1016/j.ijbiomac.2006.06.021

19. Verified

Jayakumar, R., Prabaharan, M., Reis, R. L., & Mano, J. F. (2005). Graft copolymerized chitosan—Present status and applications. *Carbohydrate Polymers*, 62(2), 142–158. https://doi.org/10.1016/j.carbpol.2005.07.017

AQ4

20. Verified

Jayakumar, R., Reis, R. L., & Mano, J. F. (2006). Chemistry and applications of phosphorylated chitin and chitosan. *E-Polymers*, 6(1). https://doi.org/10.1515/epoly.2006.6.1.447

21. Verified

Jayakumar, R., Selvamurugan, N., Nair, S. V., Tokura, S., & Tamura, H. (2008). Preparative methods of phosphorylated chitin and chitosan—An overview. *International Journal of Biological Macromolecules*, 43(3), 221–225. https://doi.org/10.1016/j.ijbiomac.2008.07.004

22. Verified

Jayakumar, R., & Tamura, H. (2006). Apatite forming ability of N-carboxymethyl chitosan gels in a simulated body fluid. *Asian Chitin Journal*, 2, 61–68.

23. Verified

Jebahi, S., Oudadesse, H., Saleh, G. B., Saoudi, M., Mesadhi, S., Rebai, T., … el Feki, H. (2014). Chitosan-based bioglass composite for bone tissue healing: Oxidative stress status and antiosteoporotic performance in a ovariectomized rat model. *Korean Journal of Chemical Engineering*, 31(9), 1616–1623. https://doi.org/10.1007/s11814-014-0072-9

24. Verified

Jiang, L., Li, Y., Wang, X., Zhang, L., Wen, J., & Gong, M. (2008). Preparation and properties of nano-hydroxyapatite/chitosan/carboxymethyl cellulose composite scaffold. *Carbohydrate Polymers*, 74(3), 680–684. https://doi.org/10.1016/j.carbpol.2008.04.035

25. Verified

Jiang, T., Nair, L. S., & Laurencen, C. T. (2006). Chitosan composites for tissue engineering: Bone tissue engineering scaffolds. *Asian Chitin Journal*, 2, 1–10.

26. Verified

Jones, J. R. (2013). Review of bioactive glass: From Hench to hybrids. *Acta Biomaterialia*, 9(1), 4457–4486. https://doi.org/10.1016/j.actbio.2012.08.023

27. Verified

Karageorgiou, V., & Kaplan, D. (2005). Porosity of 3D biomaterial scaffolds and osteogenesis. *Biomaterials*, 26(27), 5474–5491. https://doi.org/10.1016/j.biomaterials.2005.02.002

28. Verified

Kokubo, T., & Takadama, H. (2006). How useful is SBF in predicting in vivo bone bioactivity. *Biomaterials*, 27(15), 2907–2915. https://doi.org/10.1016/j.biomaterials.2006.01.017

29. Verified

Kong, L., Gao, Y., Cao, W., Gong, Y., Zhao, N., & Zhang, X. (2005). Preparation and characterization of nano-hydroxyapatite/chitosan composite scaffolds. *Journal of Biomedical Materials Research*, 75A(2), 275–282. https://doi.org/10.1002/jbm.a.30414

30. Verified

Ma, J., Wang, H., He, B., & Chen, J. (2001). A preliminary in vitro study on the fabrication and tissue engineering applications of a novel chitosan bilayer material as a scaffold of human neofetal dermal fibroblasts. *Biomaterials*, 22(4), 331–336. https://doi.org/10.1016/S0142-9612(00)00188-5

31. Verified

Madhumathi, K., Binulal, N. S., Nagahama, H., Tamura, H., Shalumon, K. T., Selvamurugan, N., … Jayakumar, R. (2009). Preparation and characterization of novel β-chitin–hydroxyapatite composite membranes for tissue engineering applications. *International Journal of Biological Macromolecules*, 44(1), 1–5. https://doi.org/10.1016/j.ijbiomac.2008.09.013

32. Verified

Mooney, D. J., Baldwin, D. F., Suh, N. P., Vacanti, J. P., & Langer, R. (1996). Novel approach to fabricate porous sponges of poly(d,l-lactic-co-glycolic acid) without the use of organic solvents. *Biomaterials*, 17(14), 1417–1422. https://doi.org/10.1016/0142-9612(96)87284-X

33. Verified

Mozafari, M., & Moztarzadeh, F. (2014). Synthesis, characterization and biocompatibility evaluation of sol–gel derived bioactive glass scaffolds prepared by freeze casting method. *Ceramics International*, 40(4), 5349–5355. https://doi.org/10.1016/j.ceramint.2013.10.115

34. Verified

Muzzarelli, R., Baldassarre, V., Conti, F., Ferrara, P., Biagini, G., Gazzanelli, G., & Vasi, V. (1988). Biological activity of chitosan: Ultrastructural study. *Biomaterials*, 9(3), 247–252. https://doi.org/10.1016/0142-9612(88)90092-0

35. Verified

Muzzarelli, R. A. A. (2009). Chitins and chitosans for the repair of wounded skin, nerve, cartilage and bone. *Carbohydrate Polymers*, 76(2), 167–182. https://doi.org/10.1016/j.carbpol.2008.11.002

36. Verified

Nam, Y. S., & Park, T. G. (1999). Porous biodegradable polymeric scaffolds prepared by thermally induced phase separation. *Journal of Biomedical Materials Research*, 47(1), 8–17. https://doi.org/10.1002/(sici)1097-4636(199910)47:1<8::aid-jbm2>3.0.co;2-l

37. Verified

Oudadesse, H., Wers, E., Bui, X. V., Roiland, C., Bureau, B., Akhiyat, I., … Pellen-Mussi, P. (2013). Chitosan effects on glass matrices evaluated by biomaterial. MAS-NMR and Biological Investigations. *Korean Journal of Chemical Engineering*, 30(9), 1775–1783. https://doi.org/10.1007/s11814-013-0104-x

38. Verified

Park, Y. J., Nam, K. H., Ha, S. J., Pai, C. M., Chung, C. P., & Lee, S. J. (1997). Porous poly(l-Lactide) membranes for guided tissue regeneration and controlled drug delivery: Membrane fabrication and characterization. *Journal of Controlled Release*, 43(2–3), 151–160. https://doi.org/10.1016/S0168-3659(96)01494-0

39. Verified

Rahaman, M. N., Day, D. E., Sonny Bal, B., Fu, Q., Jung, S. B., Bonewald, L. F., & Tomsia, A. P.(2011). Bioactive glass in tissue engineering. *Acta Biomaterialia*, 7(6), 2355–2373. https://doi.org/10.1016/j.actbio.2011.03.016

40. Verified

Schugens, C., Maquet, V., Grandfils, C., Jerome, R., & Teyssie, P. (1996b). Polylactide macroporous biodegradable implants for cell transplantation. II. Preparation of polylactide foams by liquid-liquid phase separation. *Journal of Biomedical Materials Research*, 30(4), 449–461. https://doi.org/10.1002/(SICI)1097-4636(199604)30:4<449::AID-JBM3>3.0.CO;2-P

41. Verified

Schugens, C., Maquet, V., Grandfils, C., Jerome, R., & Teyssie, P. (1996a). Biodegradable and macroporous polylactide implants for cell transplantation: 1. Preparation of macroporous polylactide supports by solid-liquid phase separation. *Polymer*, 37(6), 1027–1038. https://doi.org/10.1016/0032-3861(96)87287-9

42. Verified

Şenel, S., & McClure, S. J. (2004). Potential applications of chitosan in veterinary medicine. *Advanced Drug Delivery Reviews*, 56(10), 1467–1480. https://doi.org/10.1016/j.addr.2004.02.007

43. Verified

Seol, Y.-J., Lee, J.-Y., Park, Y.-J., Lee, Y.-M., Ku, Y., Rhyu, I.-C., … Chung, C.-P. (2004). Chitosan sponges as tissue engineering scaffolds for bone formation. *Biotechnology Letters*, 26(13), 1037–1041. https://doi.org/10.1023/B:BILE.0000032962.79531.fd

44. Verified

Silver, I. A., Deas, J., & Erecińska, M. (2001). Interactions of bioactive glasses with osteoblasts in vitro: Effects of 45S5 bioglass®, and 58S and 77S bioactive glasses on metabolism, intracellular ion concentrations and cell viability. *Biomaterials*, 22(2), 175–185. https://doi.org/10.1016/S0142-9612(00)00173-3

45. Verified

Slivka, M. A., Leatherbury, N. C., Kieswetter, K., & Niederaur, G. (2002). Porous, resorbable, fiber-reinforced scaffolds tailored for articular cartilage repair. *Tissue Engineering*, 7(6), 767–780. https://doi.org/10.1089/107632701753337717

46. Verified

Takahashi, Y., Yamamoto, M., & Tabata, Y. (2005). Osteogenic differentiation of mesenchymal stem cells in biodegradable sponges composed of gelatin and β-tricalcium phosphate. *Biomaterials*, 26(17), 3587–3596. https://doi.org/10.1016/j.biomaterials.2004.09.046

47. Verified

Webster, T. (2000). Enhanced functions of osteoblasts on nanophase ceramics. *Biomaterials*, 21(17), 1803–1810. https://doi.org/10.1016/S0142-9612(00)00075-2

48. Verified

Whang, K., Thomas, C. H., Healy, K. E., & Nuber, G. (1995). A novel method to fabricate bioabsorbable scaffolds. *Polymer*, 36(4), 837–842. https://doi.org/10.1016/0032-3861(95)93115-3

49. Verified

Yin, Y., Ye, F., Cui, J., Zhang, F., Li, X., & Yao, K. (2003). Preparation and characterization of macroporous chitosan-gelatin/β-tricalcium phosphate composite scaffolds for bone tissue engineering. *Journal of Biomedical Materials Research*, 67A(3), 844–855. https://doi.org/10.1002/jbm.a.10153

50. Verified

Zhang, Y., Venugopal, J. R., El-Turki, A., Ramakrishna, S., Su, B., & Lim, C. T. (2008). Electrospun biomimetic nanocomposite nanofibers of hydroxyapatite/chitosan for bone tissue engineering. *Biomaterials*, 29(32), 4314–4322. https://doi.org/10.1016/j.biomaterials.2008.07.038

51. Verified

Zhao, F., Grayson, W. L., Ma, T., Bunnell, B., & Lu, W. W. (2006). Effects of hydroxyapatite in 3-D chitosan–gelatin polymer network on human mesenchymal stem cell construct development. *Biomaterials*, 27(9), 1859–1867. https://doi.org/10.1016/j.biomaterials.2005.09.031

52. Verified

Zheng, J. P., Wang, C. Z., Wang, X. X., Wang, H. Y., Zhuang, H., & Yao, K. D. (2007). Preparation of biomimetic three-dimensional gelatin/montmorillonite–chitosan scaffold for tissue engineering. *Reactive and Functional Polymers*, 67(9), 780–788. https://doi.org/10.1016/j.reactfunctpolym.2006.12.002

---------- End of Document ----------

Figures

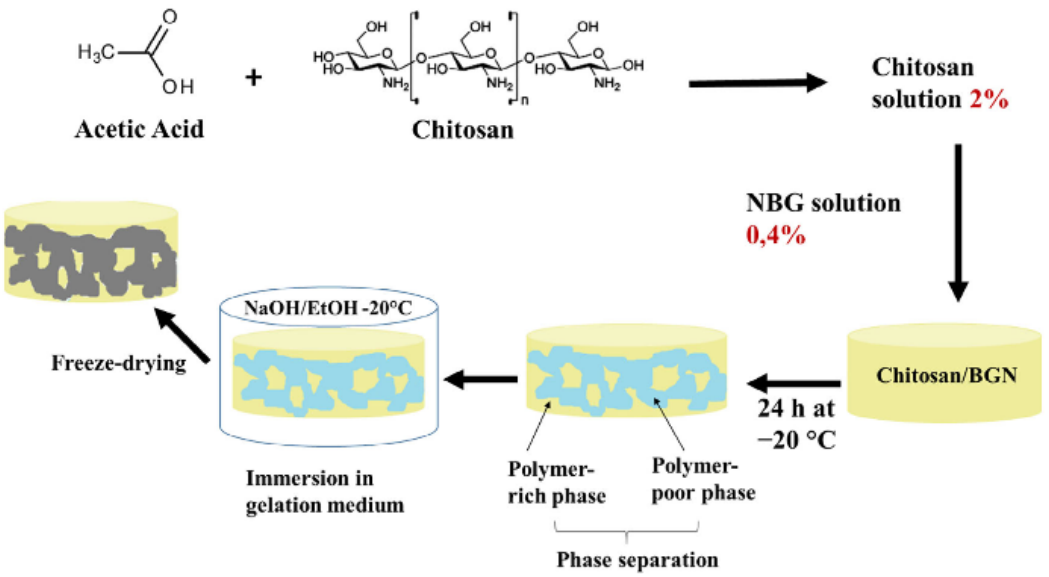

FIGURE 1 Schematic representation of bioactive glass nanoparticle (BGN)/chitosan (CH) composite scaffold fabrication method (freeze-gelation)

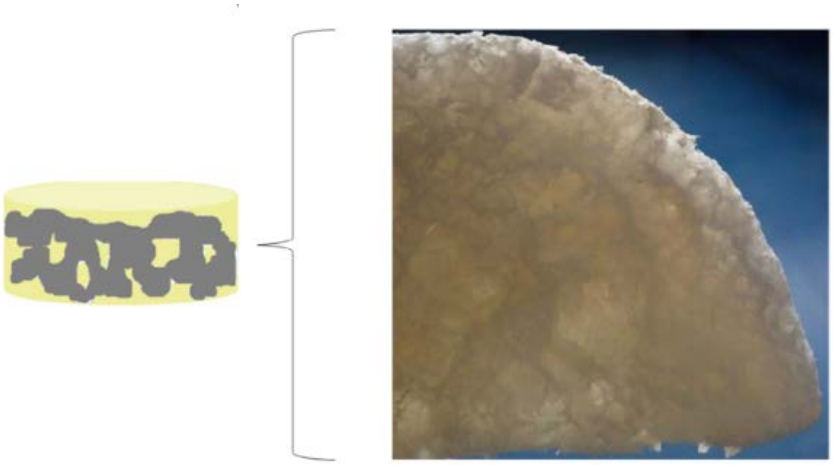

FIGURE 2 Image of the porous bioactive glass nanoparticle (BGN)/ chitosan (CH) composite scaffold prepared by the freeze-gelation method after freeze-drying

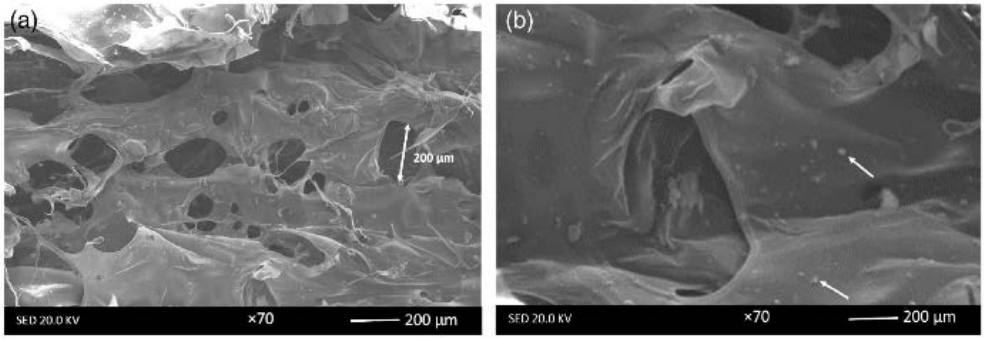

FIGURE 3 (a, b) Scanning electron micrograph (SEM) showing the macroporous structure of bioactive glass nanoparticle (BGN)/chitosan (CH) composite scaffold (a) and the dispersion of BGN in the matrix (b). Pore size is about 200 µm (b, white arrows)

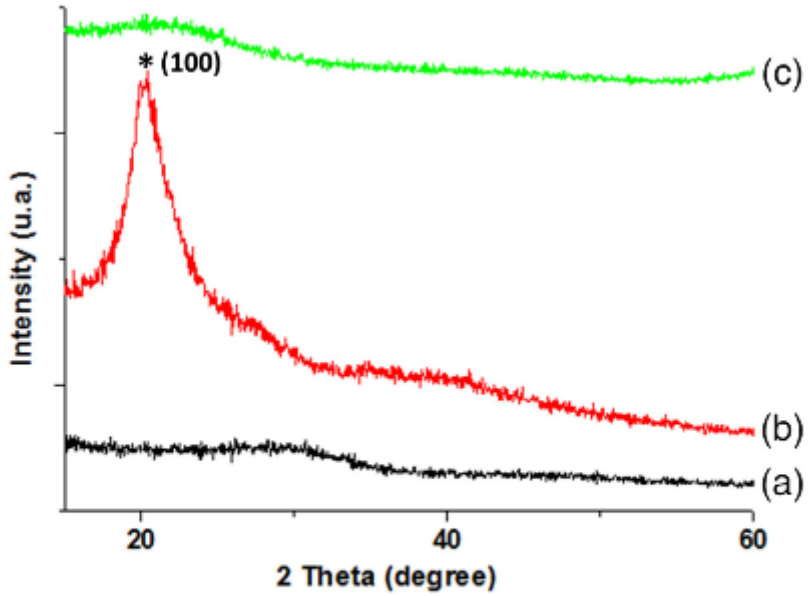

FIGURE 4 X-ray diffraction (XRD) pattern of (a) bioactive glass nanoparticle (BGN), (b) chitosan, and (c) BGN/CH composite scaffold

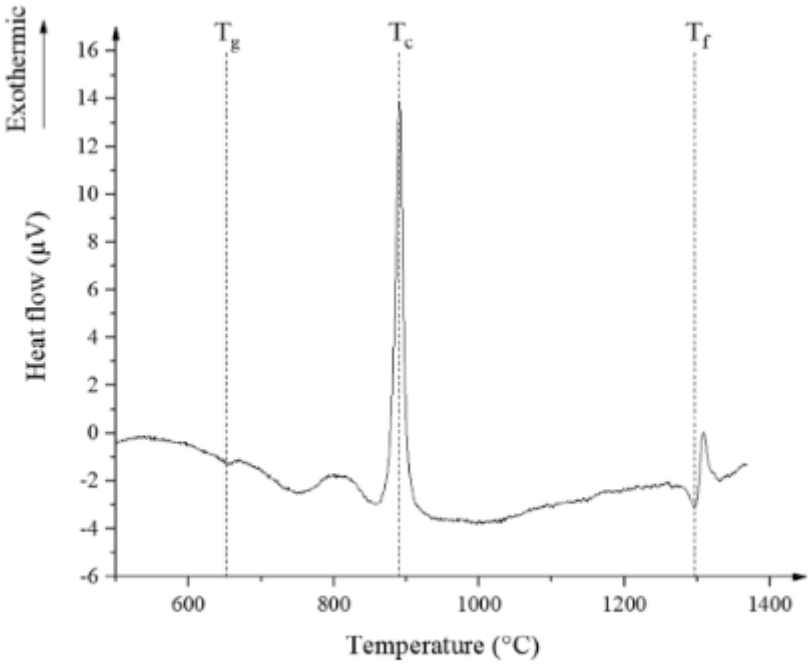

FIGURE 5 Thermal analysis (DSC) of nano bioactive glass

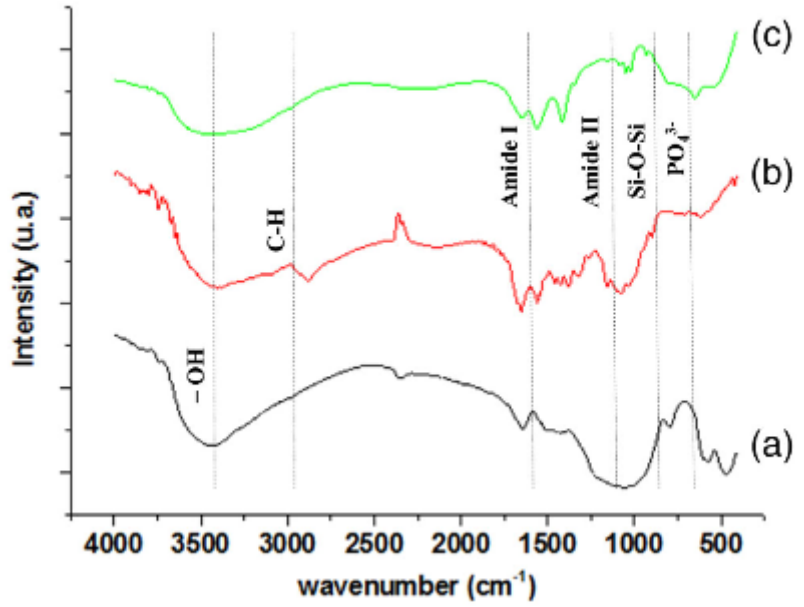

FIGURE 6 Fourier-transform infrared spectroscopy (FTIR) spectra of (a) bioactive glass nanoparticle (BGN), (b) chitosan, and (c) BGN/CH composite scaffold

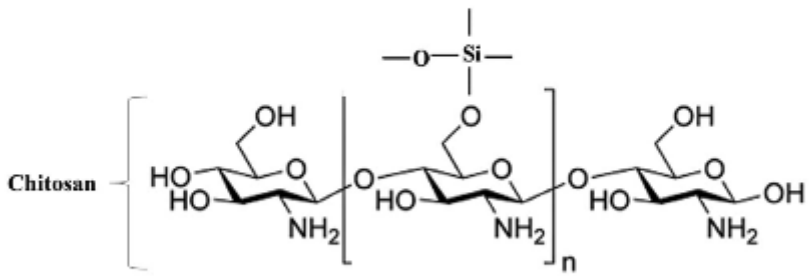

FIGURE 7 Representation of chemical interaction between chitosan and bioactive glass nanoparticles

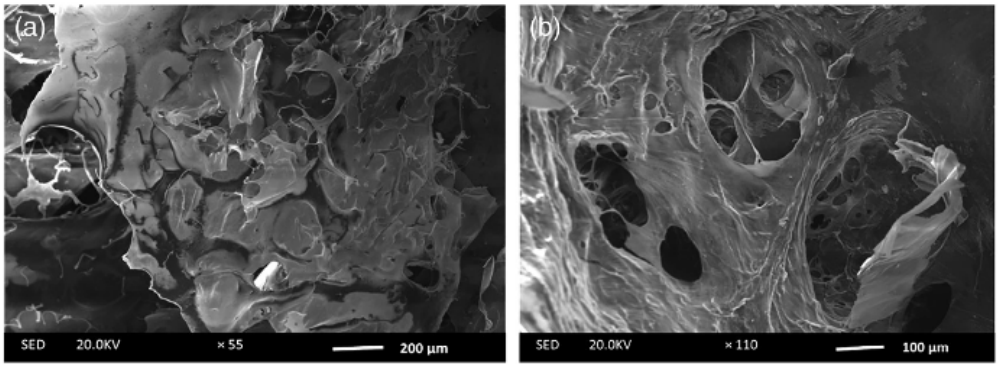

FIGURE 8 (a, b) Scanning electron micrograph (SEM) showing the structure of bioactive glass nanoparticle (BGN)/chitosan (CH) composite prepared with 2 *M* (a) and 0.5 *M* (b) of acetic acid concentration

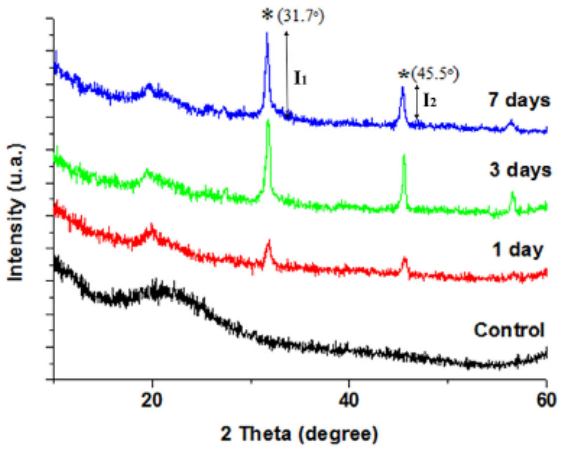

FIGURE 9 X-ray diffraction (XRD) pattern of bioactive glass nanoparticle (BGN)/chitosan (CH) composite scaffolds before and after soaking 1, 3, and 7 days in simulated body fluid (SBF)

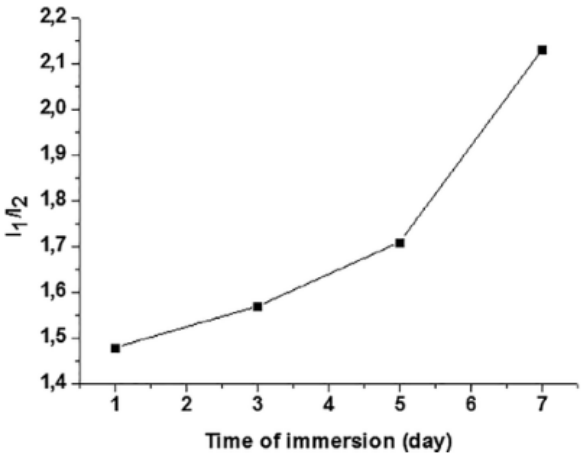

FIGURE 10 Variation of peak intensities ratio according to the immersion time of bioactive glass nanoparticle (BGN)/chitosan (CH) composite in simulated body fluid (SBF)

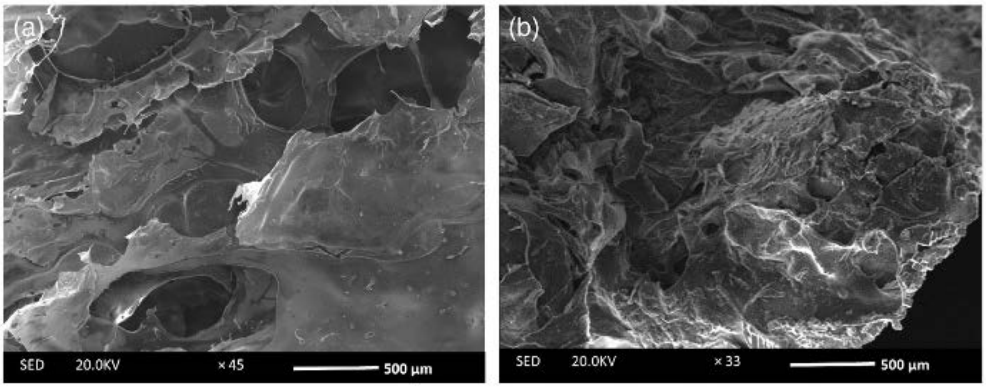

FIGURE 11 (a, b) Scanning electron micrograph (SEM) of bioactive glass nanoparticle (BGN)/chitosan (CH) composite scaffold before (a) and after 7 days of immersion in simulated body fluid (SBF) (b)

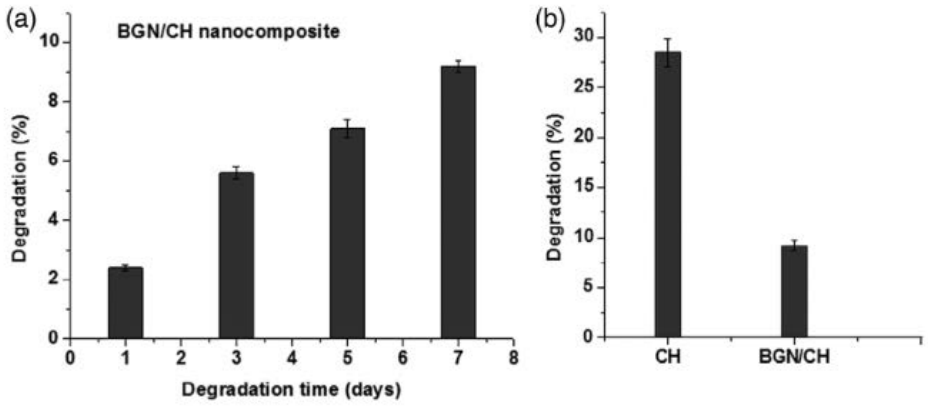

FIGURE 12 (a, b) in vitro degradation studies, which showed the degradation rate of bioactive glass nanoparticle (BGN)/chitosan (CH) nanocomposite scaffold after 7 days of immersion in phosphate-buffered saline (PBS) (a) and compared with the chitosan scaffold (b)

Tables

	Na^+	K^+	Ca^{2+}	Mg^{2+}	Cl^-	HCO_3^-	HPO_4^{2-}
SBF	142	5	2.5	1.5	148.8	4.2	1
Blood plasma	142	5	2.5	1.5	103	27	1

TABLE 1 Comparison between ion concentrations (m*M*) in SBF and in human blood plasma

TABLE 2 Chemical composition of the phosphate-buffered saline (PBS) medium

	NaCl	KCl	Na_2HPO_4	KH_2PO_4
Reagent concentration (m*M*) in PBS	137	2.7	10	1.8

TABLE 3 Surface area and porosity volume obtained by Brunauer–Emmett–Teller (BET) for the different bioactive glass nanoparticle (BGN)/chitosan (CH) composite scaffolds

BGN/CH composite	Surface area (m^2/g)	Porosity volume (mm^3/g)
BGN 20/CH	26.6 ± 0.4	7.60 ± 0.03
BGN 40/CH	25.3 ± 0.3	6.90 ± 0.04
BGN 60/CH	20.6 ± 0.4	6.70 ± 0.08
BGN 80/CH	13.8 ± 0.3	6.10 ± 0.08